Heavy inertial particles in turbulent flows gain energy slowly but lose it rapidly

Akshay Bhatnagar,[1,2,*] Anupam Gupta,[3,†] Dhrubaditya Mitra,[2,‡] and Rahul Pandit[1,§]

[1] *Centre for Condensed Matter Theory, Department of Physics, Indian Institute of Science, Bangalore 560012, India.*

[2] *Nordita, KTH Royal Institute of Technology and Stockholm University, Roslagstullsbacken 23, 10691 Stockholm, Sweden*

[3] *Mechanical Science and Engineering, University of Illinois, 1206 W. Green Street, Urbana, IL 61801, USA*

We present an extensive numerical study of the time irreversibility of the dynamics of heavy inertial particles in three-dimensional, statistically homogeneous and isotropic turbulent flows. We show that the probability density function (PDF) of the increment, $W(\tau)$, of a particle's energy over a time-scale τ is non-Gaussian, and skewed towards negative values. This implies that, on average, particles gain energy over a period of time that is longer than the duration over which they lose energy. We call this *slow gain* and *fast loss*. We find that the third moment of $W(\tau)$ scales as τ^3, for small values of τ. We show that the PDF of power-input p is negatively skewed too; we use this skewness Ir as a measure of the time-irreversibility and we demonstrate that it increases sharply with the Stokes number St, for small St; this increase slows down at St $\simeq 1$. Furthermore, we obtain the PDFs of t^+ and t^-, the times over which p has, respectively, positive or negative signs, i.e., the particle gains or loses energy. We obtain from these PDFs a direct and natural quantification of the the slow-gain and fast-loss of the particles, because these PDFs possess exponential tails, whence we infer the characteristic loss and gain times $t_{\rm loss}$ and $t_{\rm gain}$, respectively; and we obtain $t_{\rm loss} < t_{\rm gain}$, for all the cases we have considered. Finally, we show that the slow-gain in energy of the particles is equally likely in vortical or strain-dominated regions of the flow; in contrast, the fast-loss of energy occurs with greater probability in the latter than in the former.

PACS numbers: 47.27.-i,47.55.Kf,05.40.-a
Keywords: Time irreversibility

I. INTRODUCTION

Heavy inertial particles (or heavy particles) advected by turbulent flows are found in many natural phenomena and industrial processes; examples include dust particles in a storm [1], water droplets in a turbulent cloud [2], pollutant dispersions, the formation of planetesimals [3], and turbulent mixing in chemical reactions [4–8]. These heavy particles cannot be modeled as tracers because of their finite size and inertia. Many experimental, numerical, and theoretical studies have been carried out to understand the statistics of these particles in turbulent flows, [see, e.g., 9–11, for reviews]. Such a system of heavy particles also displays many intriguing features that are of interest in nonequilibrium statistical mechanics.

Some recent studies have investigated the time irreversibility of fluid turbulence by using the statistics of Lagrangian-tracer particles [12–16]. Fully-developed Navier–Stokes turbulence occurs in the limit of infinite Reynolds number or zero viscosity. The rate of energy dissipation ε does not go to zero, but it remains constant even at the highest values of the Reynolds numbers Re that have been obtained in experiments and numerical simulations. The hypothesis $\varepsilon > 0$ as Re $\to \infty$, which lies at the core of the Kolmogorov theory (K41) of turbulence, is known as the zeroth law of turbulence [17]. Fully developed forced turbulence is a nonequilibrium, statistically stationary state, which displays a constant average flux of energy from large to small length scales, where it is dissipated by viscosity. Hence, obviously, such turbulence is irreversible in time. However, this is not immediately obvious to our eyes, if we look at movies of the advection of Lagrangian tracers. By following the evolution of the kinetic energy of a single tracer particle, Ref. [13] shows that, on average, these tracers decelerate faster than they accelerate. This phenomenon of *slow-gain* and *fast-loss* of energy has been suggested to be the signature of irreversible, turbulent dynamics, in the trajectory of a single Lagrangian tracer; and it has been quantified, indirectly, in Refs. [12, 13] by the negative third moment of the probability density function (PDF) of the particle's energy increments, and the negative skewness of the PDF of the power input p to the particles by the flow. This observation suggests the violation of the principle of detailed balance in turbulent flows.

It is straightforward to understand this slow-gain and fast-loss phenomenon qualitatively via the K41 phenomenology of turbulence: The turbulent cascade in the inertial range conserves energy. The energy is injected into the fluid at the large, *integral length scale* and dissipated significantly at the small length scales that lie below the Kolmogorov dissipation scale. The eddies at the largest length scales evolve most slowly; and those at the smallest length scales are the fastest; hence, the dynamics of a single tracer particle shows the *slow-gain* and *fast-loss* features described above; and the resulting

* akshayphy@gmail.com
† anupam1509@gmail.com
‡ dhruba.mitra@gmail.com
§ rahul@iisc.ac.in

irreversibility is, therefore, related to the aforementioned separation of time-scales in turbulent flows.

We extend these ideas to heavy particles in turbulent flows by carrying out an extensive numerical study of the time irreversibility of the dynamics of heavy inertial particles in three-dimensional (3D), statistically homogeneous and isotropic turbulent flows. In addition to being advected by the time-irreversible turbulent flow, heavy particles experience a drag force that introduces an additional source of dissipation. Nevertheless, it is still impossible to distinguish visually between forward-in-time and backward-in-time trajectories of individual particles. We illustrate this in videos V1 [18] and V2 [19] for representative heavy-particle trajectories in statistically stationary turbulent flows that are homogeneous and isotropic; video V1 runs forward in time and V2 runs backwards. However, merely by looking at the two videos it is not possible to tell which one is which. Following Refs. [12, 13], which consider Lagrangian tracers, we first characterize the irreversibility of the trajectories of heavy particles by the following two quantities: (a) The energy difference of a particle across a time scale τ,

$$W(\tau) = E(t+\tau) - E(t), \tag{1}$$

where $E(t)$ is the energy per unit mass of the particle at time t; and (b) the skewness of the PDF of the power input p to the particle by the flow. We show that the probability density function (PDF) of the increment, $W(\tau)$, of a particle's energy over a time-scale τ is non-Gaussian, and skewed towards negative values. This implies that, on average, particles gain energy over a period of time that is longer than the duration over which they lose energy. We call this *slow gain* and *fast loss*. We find that the third moment of the PDF of $W(\tau)$ is negative and scales as τ^3, for small values of τ. Next, we calculate the PDFs of times over which the power p retains the same sign. In particular, we show that the PDF of p is negatively skewed; we use this skewness Ir as a measure of the time-irreversibility and and we demonstrate that it increases sharply with the particle Stokes number St (see below), for small St; this increase slows down at $\mathrm{St} \simeq 1$. Furthermore, we obtain the PDFs of t^+ and t^-, the times over which p has, respectively, positive or negative signs, i.e., the particle gains or loses energy. From these PDFs we obtain a direct and natural quantification of the slow-gain and fast-loss feature, because these PDFs possess exponential tails, whence we infer the characteristic loss and gain times $t_{\rm loss}$ and $t_{\rm gain}$, respectively. We obtain $t_{\rm loss} < t_{\rm gain}$, for all the cases we have considered. It is well-known that, in 3D turbulent flows, every point in the flow can be classified into two topological classes [20, 21]: vortical regions or saddles, which are strain-dominated, depending on whether the discriminant of the velocity-gradient-matrix is positive or negative. By using this discriminant, we show that the slow-gain in energy of the particles is equally likely in vortical or strain-dominated regions of the flow; in contrast, the fast-loss of energy occurs with greater probability in the latter than in the former.

The remainder of this paper is organized as follows. In Section II, we introduce the models we use and the numerical methods we employ to study them. Section III is devoted to a presentation of our results. We discuss our results in the concluding Sec. IV.

II. MODEL AND NUMERICAL METHODS

If the flow velocity at the position of the particle is $\boldsymbol{u}$, then the motion of a heavy particle is governed by the following equations:

$$\dot{\boldsymbol{X}} = \boldsymbol{v}, \tag{2a}$$

$$\dot{\boldsymbol{v}} = \frac{1}{\tau_{\rm p}}\left[\boldsymbol{u}(\boldsymbol{X}) - \boldsymbol{v}\right]. \tag{2b}$$

here $\boldsymbol{v}(t)$ and $\boldsymbol{X}(t)$ denote, respectively, the velocity and position of the particle at time t, and $\tau_{\rm p} = (2a^2\rho_{\rm p})/(9\nu\rho_{\rm f})$ is the Stokes or response time of the particle, with a and $\rho_{\rm p}$ the radius and material density of the particle, respectively. Equation (2) is valid if (a) the radius of the particle $a \ll \eta$, with η the Kolmogorov dissipation scale of the advecting fluid (or the particle-scale Reynolds number is very small), (b) interactions between particles are negligible, (e.g., at low number densities of particles), (c) the particle density $\rho_{\rm p} \gg \rho_{\rm f}$, the fluid density, (d) typical particle accelerations are much larger than the acceleration because of gravity, and (e) the fluid velocity is not affected by the particles.

A. Three-dimensional Navier-Stokes turbulence

We consider the motion of the particles described by Eqs. (2) in 3D, homogeneous, and isotropic turbulent flows. The velocity field $\boldsymbol{u}(\boldsymbol{x}, t)$ is obtained by solving the three-dimensional (3D), incompressible, Navier-Stokes equation, i.e.,

$$\partial_t \boldsymbol{u} + \boldsymbol{u}\cdot\boldsymbol{\nabla}\boldsymbol{u} = \nu\nabla^2\boldsymbol{u} - \boldsymbol{\nabla}p + \boldsymbol{f}, \tag{3a}$$

$$\boldsymbol{\nabla}\cdot\boldsymbol{u} = 0, \tag{3b}$$

where p, $\boldsymbol{f}$, and ν are the pressure, external force, and the kinematic viscosity, respectively. To solve Eq. (3)) numerically, we use a pseudo-spectral method [22] with periodic boundaries and the 2/3 de-aliasing rule. Table I gives the parameters for our DNSs of the 3D Navier-Stokes equation [23] The Stokes number that we use is $\mathrm{St} = \tau_{\rm p}/t_\eta$.

III. RESULTS

We first allow the flow to develop until it reaches a statistically stationary turbulent state; and then we introduce the particles. We also ignore the transients until

TABLE I. Parameters for our 3D runs **R1** and **R2** with N^3 collection points, ν the coefficient of kinematic viscosity, δt the time step, N_p the number of particles, k_{max} the largest wave number in the simulation, η and τ_η the dissipation length and time scales, respectively, λ the Taylor micro-scale, Re_λ the Taylor-micro-scale Reynolds number, I_l the integral length scale, and T_{eddy} the large-eddy turnover time.

Run	N	ν	δt	N_p	Re_λ	$k_{\max}\eta$	ϵ	η	λ	I_l	τ_η	$T_{\rm eddy}$
R1	256	3.8×10^{-3}	5×10^{-4}	$40,000$	43	1.56	0.49	1.82×10^{-2}	0.16	0.51	8.76×10^{-2}	0.49
R2	512	1.2×10^{-3}	2×10^{-4}	$100,000$	79	1.21	0.69	7.1×10^{-3}	0.08	0.47	4.18×10^{-2}	0.41

the heavy particles reach a nonequilibrium statistically stationary state, which we monitor via the temporal evolution of the total energy of the particles. In this nonequilibrium state, the PDF of any component v_k of the velocity, of a heavy particle, is a Gaussian with zero mean and a variance

$$\langle v^2\rangle \approx \frac{u_{\rm rms}^2}{1+{\rm St_T}}, \tag{4}$$

where $\rm St_T$ is the Stokes number defined with respect to the large-eddy-turnover time. The auto-correlation function $C(t)\equiv\langle v_k(0)v_k(t)\rangle/\langle v_k^2\rangle$, at large t, decays with a time scale that is shorter than the large-eddy-turnover time of the flow (see Appendix 1 for details).

As we have mentioned above, we follow the Lagrangian-tracer studies of Refs. [12, 13], and we characterize the irreversibility of the dynamical system formed by the particles by calculating the statistics of the energy increments W and the power p:

$$W(\tau)\equiv E(t+\tau)-E(t), \tag{5a}$$

$$p\equiv \boldsymbol{v}\cdot\frac{d\boldsymbol{v}}{dt}, \tag{5b}$$

where $E\equiv(1/2)\mid\boldsymbol{v}\mid^2$ is the energy-per-unit-mass.

A. Statistics of energy increments

In Fig. (1A), we plot the PDF of the energy increment, $W(\tau)$, across a time-scale τ (normalized by the dissipation time t_η), for several different values of τ and $\rm St=1$. A careful look at this figure shows that this PDF is asymmetric about zero, with an asymmetry that is most pronounced for small τ. Even for large τ, these PDFs do not approach a Gaussian distribution, as we demonstrate in Fig. (1B). In Fig. (1C) we plot the simplest characterization of the asymmetry of the PDF of $W(\tau)$, namely, its third moment $\langle W^3(\tau)/E_{\rm flow}^3\rangle$, as a function of τ, for different values of St, where the characteristic energy of the flow $E_{\rm flow}\equiv(1/2)\langle\boldsymbol{u}^2\rangle$ is used to non-dimensionalize W. As we expect [13], at small τ, the third-moment scales as τ^3, because $W(\tau)$ is smooth, so it can be Taylor expanded at small τ.

B. Statistics of the power input

We now plot in Fig. (2A), the PDF of the power-input p to the particle per-unit-mass; p is normalized by ε, the rate-of-energy-dissipation of the flow . A careful look at the figure shows that the tails of the PDF are negatively skewed; they fall off more slowly on the negative side than on the positive side. This can be quantified by plotting the skewness of these PDFs, which, following Ref. [13], we define as the irreversibility parameter:

$${\rm Ir}=\frac{\langle p^3\rangle}{\langle p^2\rangle^{3/2}}. \tag{6}$$

In Fig. (2) we plot Ir as a function of St. As $\rm St\to 0$ we expect that Ir should approach its value for Lagrangian tracers. We find that Ir remains negative for all St; in particular, its magnitude increases sharply, at small St, but this increase slows down at about $\rm St\simeq 1$.

C. Time scales of the gain and loss of energy

We now provide a direct and natural quantification of the slow-gain and fast-loss phenomenon by analyzing the time series of p as follows: Let t^+ (t^-) be the time over which p has a positive (negative) sign, i.e., the particle gains (loses) energy. These times are the first-passage times, from positive to negative values or vice versa, of the random variable p. The PDFs of such first-passage times are called persistence PDFs; if a persistence PDF has a power-law tail the exponent of the power-law is called the persistence exponent [see, e.g., 24, 25, for the use of persistence in various problems of nonequilibrium statistical mechanics]. The same idea has been used to calculate the persistence PDFs of residence times of tracers [26] and heavy inertial particles in topological structures in two dimensional [27] and 3D [28] turbulent flows.

From the time-series of p we calculate the cumulative probability distribution (CDF) of both t^+ and t^-, which we denote by Q^+ and Q^-, respectively [29] These two CDFs, for $\rm St=1$, are plotted in Fig. (3) on log-lin scales. Clearly both Q^+ and Q^- have exponential tails, with characteristic time scales $t_{\rm gain}$ and $t_{\rm loss}$, respectively. This implies that the corresponding PDFs

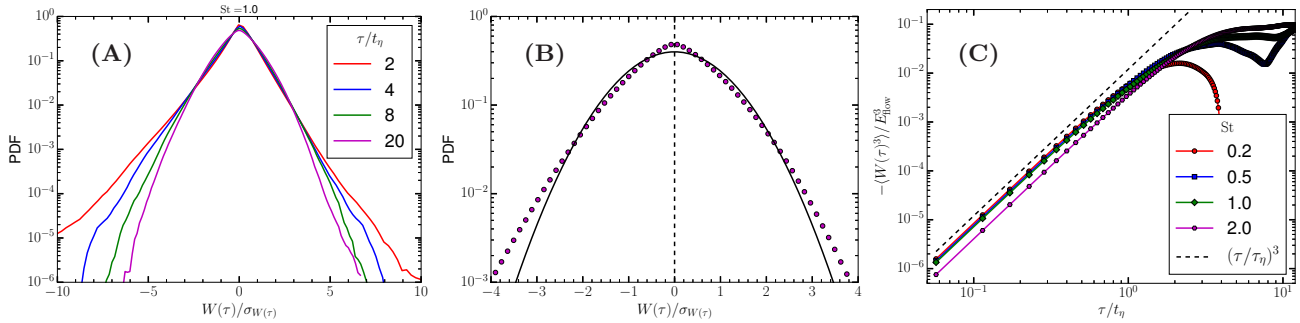

FIG. 1. (Color online) (A) Probability density functions of the energy increments, $W(\tau)$ for the different values of the time lags, τ, for St = 1. (B) Probability density function of $W(\tau)$ for $\tau = 20t_\eta$ and St = 1 (magenta circles), compared with a normal distribution with zero mean and unit variance (solid black line). (C) The third moment of the PDF of $W(\tau)$ as function of τ, for different values of St.

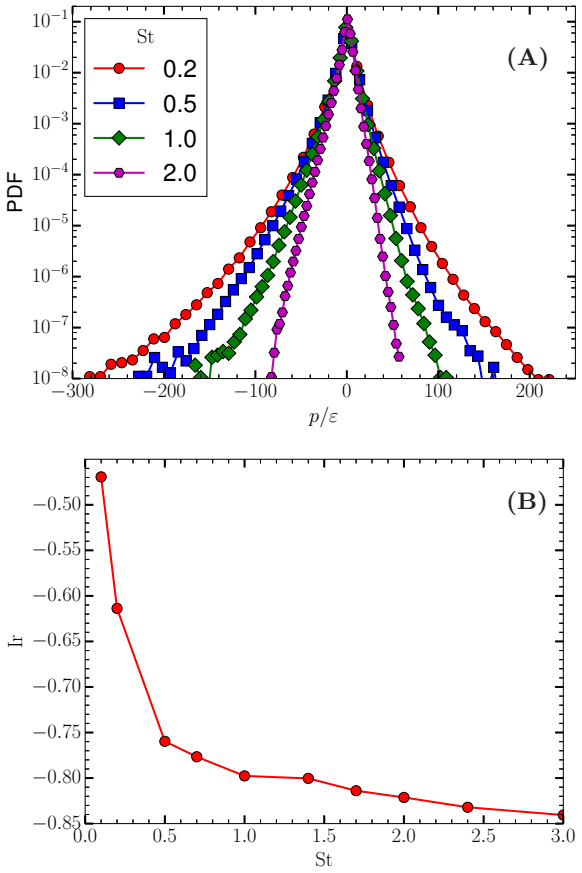

FIG. 2. (Color online) (A) The PDF of the non-dimensionalized power input p/ε to the particle by flow. (B) The measure of time irreversibility Ir, defined in Eq. (6), as a function of St.

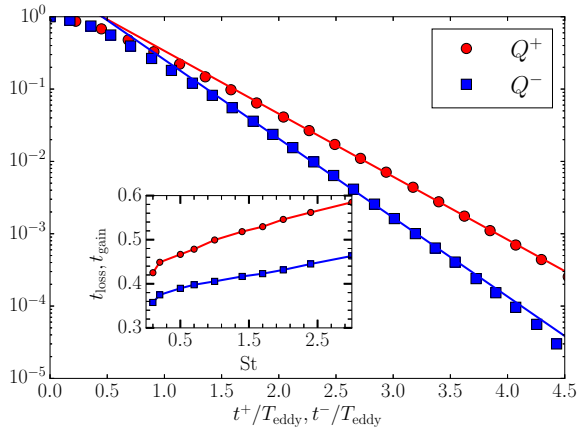

FIG. 3. (Color online) The two cumulative PDFs, Q^+ and Q^-, of the times for which the p remains respectively positive (red) and negative (blue), for St = 1. The two straight lines are linear fits to the tail of the data. The slope of these straight lines are $t_{\rm gain}$ and $t_{\rm loss}$. These are plotted as a function of St in the inset, $t_{\rm gain}$ (red circles) and $t_{\rm loss}$ (blue squares). These time scales are scaled by large eddy turn over time of the flow $T_{\rm eddy}$.

also possess exponential tails, with the same characteristic time scales. These two time scales are plotted, as functions of St, in the inset of Fig. (3), from which we infer that, for all St, $t_{\rm gain} < t_{\rm loss}$, which is a natural quantification of the slow-gain and fast-loss feature.

D. Irreversibility and the topology of the flow

The topology of a 3D vector field can be characterized by its gradient-matrix. A 3×3 matrix, $\mathcal{B}$ has three invariants, namely, its trace $\mathrm{Tr}\,\mathcal{B} = \lambda_1 + \lambda_2 + \lambda_3$, $Q \equiv \lambda_1\lambda_2 + \lambda_2\lambda_3 + \lambda_3\lambda_1$, and its determinant $\mathrm{Det}\,\mathcal{B} = \lambda_1\lambda_2\lambda_3$, where λ_1, λ_2, and λ_3 the are three eigenvalues of $\mathcal{B}$. If the vector field is incompressible, like our flow velocity field, there are only two invariants, because the trace of the velocity-gradient matrix is zero everywhere. We consider incompressible turbulent flows, so the velocity-

gradient matrix is a random matrix with zero trace; it is conventional [21] to denote its two invariants by the symbols Q and $R \equiv -\mathrm{Det}\,\mathcal{B}$. Depending on the values of Q and R, four different types of flow topologies are possible: two are elliptic (or vortical) points, with a third stable/unstable direction, and two are saddles, with axial or bi-axial strain. Whether the flow at a point is a topological vortex or a saddle depends on the sign of the discriminant, $\Delta \equiv (27/4)R^2 + Q^3$, of the characteristic equation of the velocity-gradient matrix; it is positive in vortical regions and negative in strain-dominated saddles. We have argued above that the particles lose energy to fast, small-length-scale eddies and gain energy from large-length-scale eddies. The topological structures are small-length-scale properties; hence, by the usual assumption of length-scale-separation in turbulence, we expect that the gain in energy, which occurs in large-scale eddies, does not depend on the topology of the flow. By contrast, the loss in energy occurs in small-length-scale eddies, which are intimately connected with the topological structures we have described above. It has been established recently that heavy particles, in 3D turbulent flows, spend more time in strain-dominated regions than in vortical regions [28]; consequently, we expect that the loss of energy occurs more in strain-dominated regions than in vortical regions in the flow. To check the validity of this expectation, we plot, in the top panel of Fig. (4), the PDFs of p, obtained separately from regions with saddles and vortices. There is no distinction between these two PDFs for positive p, i.e., when the particles gain energy. By contrast, when p is negative, i.e., when the particles lose energy, this loss is more likely to occur in strain-dominated flow regions than in vortical ones. This is also confirmed in the bottom panel of Fig. (4), where we plot the contribution to the irreversibility parameter Ir, obtained separately from vortical and strain-dominated regions, for several different values of St; in particular, the contribution from the vortices is significantly smaller than that from the saddles, which shows that the dominant contribution to the skewness of the PDF of the power comes from the saddles.

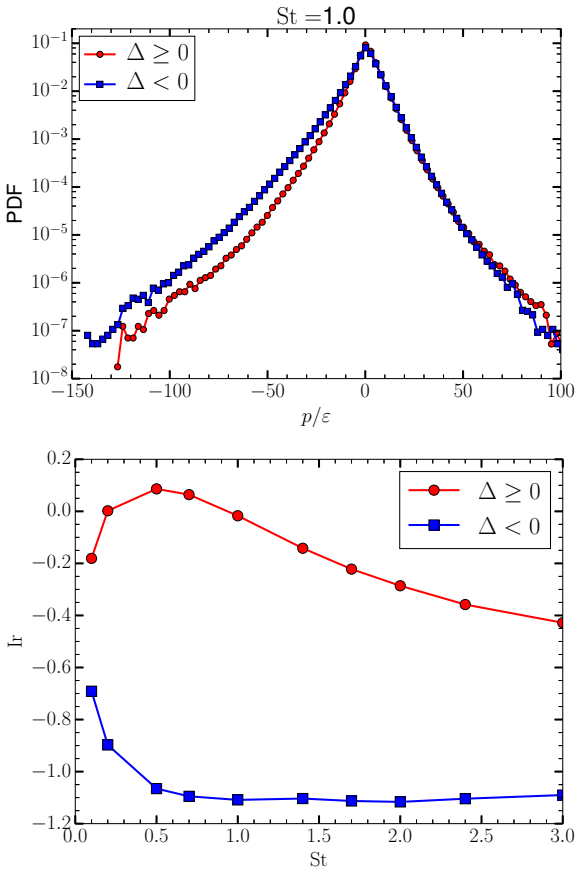

FIG. 4. (Color online) (top panel) The PDFs of the non-dimensionalized power input p/ε obtained separately from vortical (red) and strain-dominated (blue) regions of the flow, for St = 1. (bottom panel) Contributions to the irreversibility parameter Ir from vortical (red) and strain-dominated (blue) regions of the flow.

IV. CONCLUSIONS

We have carried out a detailed numerical study of the time irreversibility of the dynamics of heavy particles in 3D, statistically homogeneous and isotropic turbulent flows. We have shown that these particles, which follow Eq. (2), reach nonequilibrium statistically stationary states. We have characterize these states by calculating variety of PDFs and auto-correlation functions. The simplest of these are PDFs and auto-correlation functions of the velocity components; we have shown that these PDFs are close to Gaussian. We have also computed the PDFs of the increments of the particle's energy $W(\tau)$, for different values of τ, and shown that these PDFs are non-Gaussian and skewed towards negative values. This implies that, on average, particles gain energy over a period of time that is longer than the duration over which they lose energy. For passive Lagrangian tracers, this phenomenon, has been called a flight-crash effect in Ref. [13]; we simply refer to it as slow gain and fast loss. We have also found that the third moment of $W(\tau)$ scales as $\sim \tau^3$, at small values of τ.

We have computed the PDFs of the scaled power input p, for different values of St, and shown that it is negatively skewed. This negative skewness provides us a measure of the time irreversibility Ir. We have demonstrated that the magnitude of Ir increases with St, sharply for small St, but more slowly thereafter (at about St ≈ 1). These qualitative features can also be captured by models in which the flow velocity is obtained from stochastic models with non-zero correlation time [30].

Our study has led to a direct and natural measure of the slow-gain and fast-loss of energy. Specifically, we have calculated the PDFs of t^+ and t^-, the times over which p has, respectively, positive or negative signs. These PDFs

have exponential tails, from which we have inferred the characteristic loss and gain times $t_{\rm loss}$ and $t_{\rm gain}$, respectively. We have shown $t_{\rm loss} < t_{\rm gain}$, for all the values of St we have considered. Furthermore, we have shown that the slow-gain in energy of the particles is equally likely in vortical or strain-dominated regions of the flow; in contrast, the fast-loss of energy occurs with greater probability in the latter than in the former.

Time irreversibility for Lagrangian tracers, advected by turbulent flows, arises solely because of the time-irreversible nature of such flows. In contrast, for the case of heavy particles, time irreversibility arises because of two reasons: (a) turbulent flows, which advect such particles, are irreversible; and (b) the Stokes drag, exerted by the flow on the particle, is dissipative. The separation of the effects of particle inertia and turbulence on time irreversibility is non-trivial. Our study has shown how the effect of inertia can be captured clearly by the dependence of Ir on St, which we have shown in Fig. 2.

The time irreversibility for Lagrangian tracers, advected by turbulent flows, has been studied theoretically, numerically, and experimentally (see, e.g., Refs. [12, 13]). Our study has carried out analogous theoretical and numerical studies for heavy particles advected by turbulent flows; and we have obtained clear signatures for such irreversibility, which can be measured in heavy-particle-laden flows. We hope, therefore, that our studies will stimulate experimental investigations of time irreversibility in such heavy-particle-laden flows.

V. ACKNOWLEDGMENTS

This work has been supported in part by the Swedish Research Council under grants 2011-542 and 638-2013-9243 (DM), Knut and Alice Wallenberg Foundation (DM and AB) under the project Bottlenecks for particle growth in turbulent aerosols (Dnr. KAW 2014.0048), Council of Scientific and Industrial Research (CSIR), University Grants Commission (UGC), and Department of Science and Technogy (DST India) (AB and RP). We thank SERC (IISc) for providing computational resources. DM thanks the Indian Institute of Science for hospitality during the time some of these calculations were initiated. RP thanks NORDITA for hospitality during the period in which this paper was being written. We thank Prasad Perlekar and Samriddhi Shankar Ray for useful discussions.

[1] J. F. Kok, E. J. Parteli, T. I. Michaels, and D. B. Karam, Reports on Progress in Physics **75**, 106901 (2012).
[2] H. Pruppacher and J. Klett, Microphysics of Clouds and Precipitation (Springer Science & Business Media, 2010), Vol. 18.
[3] P. J. Armitage, Astrophysics of Planet Formation (Cambridge University Press, Cambridge, UK, 2010).
[4] J. H. Sienfeld, Willey Interscience, New York **738**, (1986).
[5] G. Csanady, Turbulent Diffusion in the Environment, volume 3 of Geophysics and Astrophysics Monographs, D, 1976.
[6] A. Bracco, P. Chavanis, A. Provenzale, and E. Spiegel, Physics of Fluids (1994-present) **11**, 2280 (1999).
[7] M. Pinsky and A. Khain, Journal of aerosol science **28**, 1177 (1997).
[8] B. Rothschild and T. Osborn, Journal of Plankton Research **10**, 465 (1988).
[9] F. Toschi and E. Bodenschatz, Annual Review of Fluid Mechanics **41**, 375 (2009).
[10] K. Gustavsson and B. Mehlig, Advances in Physics **65**, 1 (2016).
[11] A. Pumir and M. Wilkinson, Annual Review of Condensed Matter Physics **7**, 141 (2016).
[12] H. Xu *et al.*, arXiv preprint arXiv:1310.5006 (2013).
[13] H. Xu *et al.*, Proceedings of the National Academy of Sciences **111**, 7558 (2014).
[14] E. Lévêque and A. Naso, EPL (Europhysics Letters) **108**, 54004 (2014).
[15] T. Grafke, A. Frishman, and G. Falkovich, Physical Review E **91**, 043022 (2015).
[16] M. Cencini, L. Biferale, G. Boffetta, and M. De Pietro, Physical Review Fluids **2**, 104604 (2017).
[17] U. Frisch, Turbulence the legacy of A.N. Kolmogorov (Cambridge University Press, Cambridge, 1996).
[18] `https://www.youtube.com/watch?v=6NUDcTaexew`.
[19] `https://www.youtube.com/watch?v=FNWitXHnJuA&feature=youtu.b`
[20] A. E. Perry and M. S. Chong, Annual Review of Fluid Mechanics **19**, 125 (1987).
[21] M. Chong, A. Perry, and B. Cantwell, Phys. Fluids. A **3**, 765 (1990).
[22] C. Canuto, M. Hussaini, A. Quarteroni, and T. Zang, Spectral methods in Fluid Dynamics (Spinger-Verlag, Berlin, 1988).
[23] Note that the value of Re_λ given in Table I is smaller as compared to that in other studies reported in the literature for the same resolution, e.g., Ref [31, 32]. This is because, in these studies, the expression for λ contains an extra factor of $\sqrt{5}$ relative to our definition.
[24] S. Majumdar, Curr. Sci. **77**, 370 (1999).
[25] A. Bray, S. Majumdar, and G. Schehr, Advances in Physics (2013).
[26] P. Perlekar, S. Ray, D. Mitra, and R. Pandit, Phys. Rev. Lett **106**, 054501 (2011).
[27] A. Gupta, D. Mitra, P. Perlekar, and R. Pandit, arXiv preprint arXiv:1402.7058 (2014).
[28] A. Bhatnagar *et al.*, Physical Review E **94**, 063112 (2016).
[29] It is generally difficult to obtain reliable information about the tail of a PDF by plotting histograms because of possible binning errors. Hence, instead of studying the tail of the PDF, we have calculated the CDF of the power of the particles by using the rank-order method [33] that

leads to the CDF that is free from binning errors. By definition, the CDF of a random variable s is given by $Q(s) \equiv \int_0^s P(s)ds$, where P and Q are, respectively, the probability density function and the cumulative distribution function. To calculate the CDF of a data set, with N samples, via the rank-order method, we sort the data in *decreasing* order, assign the maximum value rank 1, the next value rank 2, and so on. The quantity we plot on the vertical axis of Fig. (3) is this rank divided by the sample size N. Clearly, this is $1 - Q(s)$. This method is best suited to the study of the tails of the CDF. If we are interested in the behavior of the CDF for small values of its arguments, it we sort the data in *increasing* order and then apply the method described above.

[30] A. Bhatnagar, Ph.D. thesis (unpublished), Dept. of Physics, Indian Institute of Science, Bangalore, 2016.

[31] H. Yoshimoto and S. Goto, Journal of Fluid Mechanics **577**, 275 (2007).

[32] J. Bec *et al.*, Journal of Fluid Mechanics **550**, 349 (2006).

[33] D. Mitra, J. Bec, R. Pandit, and U. Frisch, Phys. Rev. Lett **94**, 194501 (2005).

1. Characterization of the statistically stationary turbulent state

In Fig. 5 we show plots, of PDFs of x component v_x of the velocity of the particle (left panel). These PDFs are close to a Gaussian distribution. (middle panel) Shows the mean of v^2 plotted as a function of the Stokes-number defined, by $T_{\rm eddy}$, as $\mathrm{St_T} = \tau_{\rm p}/T_{\rm eddy}$; the black solid line shows the plot of $\langle u^2 \rangle/(1 + \mathrm{St_T})$ as a function of $\mathrm{St_T}$. (right panel) of Fig. (5) shows the auto-correlation function

$$C(t) \equiv \frac{\langle v_x(t) v_x(0) \rangle}{\langle v_x^2 \rangle} \tag{7}$$

of the x component of $\boldsymbol{v}$. The auto-correlation functions decay at large times. The characteristic decay time decreases with St.

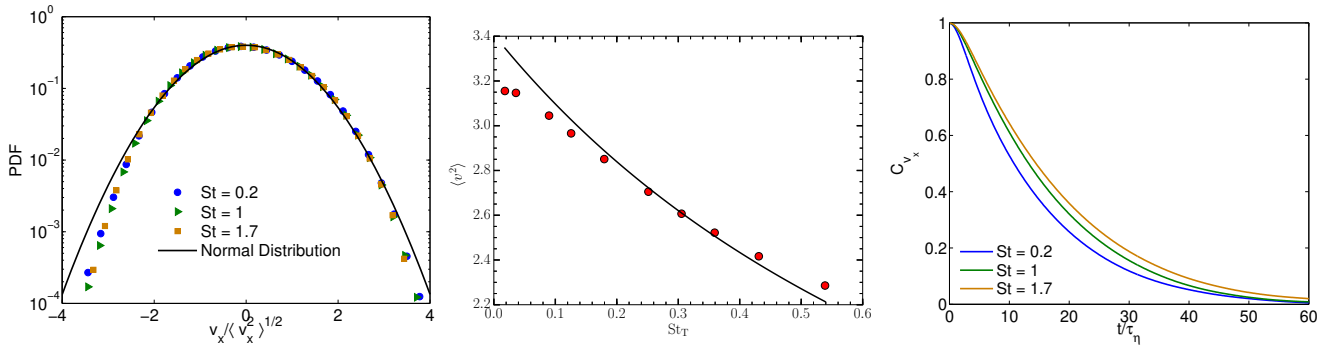

FIG. 5. (Color online) (left panel) The PDFs of the x component of the velocity of the particle. The black solid line shows a normal distribution with mean zero and standard deviation unity. (middle panel) The mean of v^2 plotted as a function of the Stokes-number defined, by $T_{\rm eddy}$, as $\mathrm{St_T} = \tau_{\rm p}/T_{\rm eddy}$; the black solid line shows the plot of $\langle u^2 \rangle/(1+\mathrm{St_T})$ as a function of $\mathrm{St_T}$. (right panel) The auto-correlation function C_{v_x} of the x component of the velocity of the particle.